

1
2
3
4
5
6
7
8
9
10
11
12
13
14
15
16
17
18
19
20
21

Chapter X

Comprehensive dynamical models of global and regional water isotope distributions

David Noone

*Department of Atmospheric and Oceanic Sciences, and
Cooperative Institute for Research in Environmental Sciences,
University of Colorado
Boulder, CO, USA*

(Email: dcn@colorado.edu Phone: +1 303 735-6073)

and

Christophe Sturm

*Bert Bolin Centre for Climate Research
Institute for Geology and Geochemistry
Stockholm University
Stockholm, Sweden*

(Email: Christophe.Sturm@geo.su.se Phone: +46 8 16-4723)

Revision 1: 15 January 2009

Revision 2: 17 February 2009

22 **Abstract**

23 Water isotope tracers can be included in comprehensive atmospheric models and can
24 provide deeper insight to isotope distributions than simple physically-based isotope
25 models or statistical methods because of their ability to resolve the underlying processes
26 of interest. Within such models, isotope tracers follow normal “prognostic” water, and
27 differ only in that fractionation is applied during surface evaporation and transpiration,
28 cloud condensation processes, exchange between falling raindrops and environmental air,
29 and when there are any extra water sources. The details of the mass balance that underlies
30 modeling isotopes and the key processes can be represented in models are examined to
31 illuminate how it is the compilation of many simple aspects which give rise to a
32 comprehensive model. One particular advantage of dynamical isotope models is their
33 ability to account for mixing of air masses by resolved larger-scale transport and by
34 smaller scale parameterized turbulence. While the output from comprehensive dynamical
35 isotope models is useful for subsequent applications, adequate accounting for model error
36 is needed. In the past, few observations have been available to validate isotopic models,
37 especially for vapor which is the model state variable of importance, and validating
38 models remains a limitation. Nonetheless, comprehensive models are valuable in
39 mapping water isotope distributions in vapor and precipitation. They are also well suited
40 to diagnostic studies in which model sensitivity tests expose the physical basis for the
41 final isotopic signal. This type of analysis is invaluable in guiding the interpretation of
42 isotopic observations.

43 **Introduction**

44 Unlike statistical maps of water isotope distributions, the isotope distributions that
45 emerge from numerical simulations with comprehensive mechanistic models reflect an
46 understanding of the underlying physical and chemical processes which control the
47 budgets of water and water isotopologues. A comprehensive model accounts for all
48 processes which are determined to be, or likely to be, of significant influence on the
49 budgets (e.g., transpiration, cloud formation and rain, oxidation of various chemical
50 agents). Dynamical models, such as weather and climate models, are particularly
51 advantageous for isotope studies because the often non-linear and non-local influences of
52 transport processes can be accounted for in simulation. The final isotope distribution
53 emerges from numerical integration of the budget equation, yet the result holds
54 advantages over statistical maps because the mechanistic cause of the distribution can be
55 determined quantitatively by examining additional diagnostics on all the contributions of
56 each of the controlling processes computed by the model. In this way comprehensive
57 dynamical models of water isotopologues can provide maps of isotope concentration that
58 compliment those obtained by statistical methods. Here we provide a basis for
59 understanding how water isotope distribution can be simulated by incorporating isotope
60 fractionation schemes into the water cycles of weather and climate models.

61

62 Comprehensive models can be distinguished from simpler models that appear frequently
63 in isotope studies. Simple models such as those of trajectory and box budget-types (which
64 includes Rayleigh models and simple mixing models) are extremely valuable at providing
65 first order descriptions of water isotope distributions. However, they are limited in three

66 important regards: 1) They often need appropriate initial conditions to be provided, 2)
67 they require gross simplification of cloud and other exchange processes, and 3) they
68 seldom account for mixing and transport of air masses in any detail. More comprehensive
69 isotope models, such as those provided through modification of atmospheric general
70 circulation models (GCMs) or regional meteorological models to include isotope tracers,
71 can overcome some of these problems. To illustrate this, the basis of isotope tracking
72 schemes as employed in comprehensive dynamical models is described and some
73 examples of the use of such models in both reproducing climatological distributions and
74 in informing process studies are discussed. Since the underpinning of comprehensive
75 models is numerically evaluating the processes which contribute to the budgets, we
76 describe in some detail the basic budget constraints and how account is made of the
77 pertinent exchange processes. While models exist which can resolve exchanges at
78 molecular scales and motions at turbulent scales, and some of these have been tasked
79 with modeling isotopes, we focus here on dynamical models with grid resolution in the
80 range 20-500 km.

81

82 **X.1 Development and uses of comprehensive isotope models**

83 In the early 1980s the Laboratoire de Météorologie Dynamique (LMD) atmospheric
84 GCM was fitted with water isotope tracers with the technique obtaining notoriety with
85 the seminal paper published in Nature (Joussaume et al. 1984). This work demonstrated
86 that a global model with even modest representation of the atmospheric water cycle can
87 reproduce the bulk features of the global and seasonal variations in isotopic composition
88 in precipitation. Shortly after, J. Jouzel spent sabbatical time in New York and working

89 with the modeling group at the Goddard Institute for Space Sciences developed an
90 isotope scheme in that group's global model (Jouzel et al. 1987; Jouzel et al. 1991).
91 Initially, early studies focused on testing the validity of water isotopes as climate proxies.
92 Indeed Joussaume's early work included simulating dust concentrations such that results
93 could also validate proxy reconstructions from ice core dust records (Joussaume 1993;
94 Joussaume and Jouzel 1993). The interest in using comprehensive models to simulate
95 isotope distributions in precipitation and vapor has continued to grow with numerous
96 models now having isotopic tracers (Table 1). Intriguingly, the development of isotope
97 schemes in models has often been the result of doctoral studies (Joussaume 1983;
98 Hoffmann 1995; Noone 2001; Werner and Heimann 2002; Lee 2005; Sturm 2005; Risi et
99 al. 2008).

100

101 While initially ice core records were of interest, and the validation of the so-called
102 isotope-temperature slope, the community's attention quickly moved to other aspects of
103 the isotope hydrology. Research areas include the monsoons (Hoffmann and Heimann
104 1997; Sturm et al. 2007a; Sturm et al. 2007b), tropical corals (Cole et al. 1999; Charles et
105 al. 2001; Brown et al. 2006), atmospheric transport processes (Noone and Simmonds
106 2002a; Vuille et al. 2003) and cloud processes (Schmidt et al. 2005; Lee et al. 2007).
107 Still, because of the great experience with isotopes in the paleoclimate community, many
108 of the published studies using water isotopes in comprehensive dynamical models have
109 focused on examining past climate. There has been less attention given to using
110 dynamical models of water isotopes to describe modern climate change, although the

111 studies of Hoffmann et al. (2000), Schmidt et al. (2007) and Yoshimura et al. (2008)
112 stand as exceptions.
113
114 The non-isotope modeling community often sees the utility isotopes as informing the
115 construction of more accurate cloud microphysical packages for non-isotopic models, yet
116 there has been little work in this area. Part of the reason for the lack of engagement is that
117 there is rarely a perceived clear advantage in considering isotopic exchange, and in part
118 that existing isotope models in fact only poorly constrain the detailed microphysics used
119 in modern dynamical models. This is in part due to lack of an adequate amount of
120 isotopic data for validation. Nonetheless a number of studies with comprehensive
121 dynamical isotope models have informed understating of cloud processes in the
122 underlying hydrology. As a case in point, Schmidt et al. (2005) aimed to explain the
123 impact on the isotope distribution from different assumptions about cumulous clouds in
124 the context of explaining the aircraft observations of Webster and Heymsfield (2003).
125 Similarly, Bony and Risi (2008) used a parameterized model of convection (in an off-line
126 configuration rather than coupled to a dynamical model) to explain the role of cloud
127 microphysics in setting the isotopic composition of the tropics. So too, Lee et al. (2008)
128 and Risi et al. (2008) targeted the impact of post condensation processes on the isotopic
129 composition of precipitation. These studies demonstrate the utility in reconsidering the
130 simulated hydrology by examining the impact on the isotopic results. To do so, however,
131 requires an isotopic scheme that is designed and implemented with this as its objectives.
132

133 **X.2 Isotopic budgets in comprehensive models**

134 While it is often that diagnostics on the isotopic composition of precipitation or
135 evaporation that results from models which of most interest, the state variable of interest
136 in atmospheric models is the water vapor abundance. Usually this is quantified by mass
137 mixing ratio or specific humidity (q)¹. Modern climate models also include state variables
138 for cloud liquid and ice and land surface components of global and regional models track
139 the amount of water in soil, snow and sea ice. The isotopic composition of all these and
140 any other state variables must be tracked to develop a comprehensive closed isotope
141 scheme.

142

143 The water cycle in a dynamical model stems from the prediction of water vapor mixing
144 ratio (q), and is described by the evaluation of the tendency equation:

145
$$\frac{\partial q}{\partial t} = \underbrace{-\mathbf{V} \cdot \nabla q}_{(1)} + \underbrace{D \nabla_h^2 q}_{(2)} + \underbrace{\frac{\partial}{\partial p}(\overline{\omega' q'})}_{(3)} + E - C + S. \quad (\text{X.1})$$

146

147 The first three terms on the right (numbered 1-3) warrant discussion. The three-
148 dimensional wind field is \mathbf{V} , and the first term on the right ($-\mathbf{V} \cdot \nabla q$) is the large-scale
149 advective transport in a coordinate system (e.g., x, y, p , where p is pressure and the
150 velocity in the vertical is ω). Here, “large-scale” can be defined as that which can be
151 resolved by the model, and is a function of the model resolution. Horizontal transport by

¹ Strictly the isotope ratio is the mole ratio of heavy to light isotopes, so one should use volume mixing ratio, which differs only by a constant (ratio of molecular weight of air and the vapor).

152 smaller scale motions is expressed in the characteristic form of horizontal diffusion (i.e.,
153 $D\nabla_h^2 q$) with some, generally non-linear, effective eddy diffusion coefficient D . The third
154 term on the right captures vertical transports due to small scale processes, and is
155 expressed mathematically as associated with the Reynolds stress $\omega'q'$. Such processes are
156 not resolved in models, yet the effects of the processes are important. As such they are
157 accounted for through “parameterization,” which aims to estimate the effects of small
158 scale processes on the large-scale quantities using only large-scale information. Should
159 the vertical transport be associated with (dry) turbulent motions the third term takes the
160 meaning of turbulent flux, such as one finds most strongly in the boundary layer. On the
161 other hand, if the turbulence occurs in concert with condensation, this term captures
162 transport in the region of convective clouds, in which there may be water entrained at
163 their base and detrained at some higher altitude. Accounting for both boundary layer
164 turbulence and moist convection is a topic great interest in dynamical modeling, and a
165 complex subject in its own right. It is appropriate to note here, however, that the sum of
166 these three numbered terms in (X.1) capture the total transport and mixing of air masses,
167 and it is the explicit evaluation of them which is a unique element of dynamical models.

168

169 Beyond transport, the water budget has both active sources and sinks. The primary source
170 of water in the atmosphere is evaporation and evapo-transpiration at the surface and
171 evaporation of falling hydrometeors, E . Loss of water is via condensation, C . The
172 additional term, S , accounts for sources or sinks which are associated with other
173 processes, and can include the water source associated with methane oxidation in the
174 stratosphere (e.g., McCarthy et al. 2004), mass independent isotopic exchange in the

175 region of the ozone layer (e.g., Yung and Miller 1997), and radioactive decay, in the case
176 of, say, ^{19}O or ^3H .

177

178 A comprehensive model for to simulation isotopic composition stems from writing down
179 an analog of the atmosphere budget (X.1) for isotopologues and considering their
180 changes relative to the most abundant nuclide. The challenge in developing an isotope
181 model is seen by noting that where condensation and evaporation occur, it does so with
182 both kinetic and equilibrium fractionation, and the additional sources typically have
183 different isotopic signatures. Thus the terms E, C and S need special attention because it
184 is the isotopic variation in these which give rise to isotope distributions. The transport
185 processes themselves do not impose fractionation (since there is no phase change), but
186 the details of transport are fundamental in setting the spatial and temporal distributions.
187 However, since the key strength of comprehensive models is in accounting for transport
188 and mixing processes, they warrant further examination.

189

190 **X.3 Transport processes and numerical solution**

191 *X.3.1 Diagnostic water tracers*

192 Before examining the details of isotopic calculations, it is useful to consider the more
193 abstract idea of water tracers. The use of non-fractionating water tracers is greatly
194 advantageous in diagnosing water transport pathways in the atmosphere, and tracking
195 specific water origins (Koster et al. 1986; Koster et al. 1993; Bosilovich and Schubert
196 2002; Noone and Simmonds 2002a). Indeed the desire to use isotopes in diagnostic

197 studies often stems from their ability to naturally tag water sources. Water tracers can be
 198 defined by duplicating the water budget equation, (X.1), such that within the model
 199 “tracer water” follows the usual “prognostic water” exactly. The difference between
 200 tracer water and prognostic water is only that the latter influences the diabatic heating,
 201 and the former is purely a slave to the prognostically computed quantity. At a coding
 202 level this is easily (but often tediously) achieved by replicating lines of code for the tracer
 203 water whenever the prognostic water variable is modified. Denoted with subscript i , the
 204 tracer water budget is

$$205 \quad \frac{\partial q_i}{\partial t} = -\mathbf{V} \cdot \nabla q_i + D\nabla_h^2 q_i + \frac{\partial}{\partial p}(\overline{\omega' q_i'}) + R_E E - R_C C + R_S S, \quad (\text{X.2})$$

206 which conserves the tracer proportion during transport, and the ratio of tracer to total
 207 (prognostic) water is given via the source terms and the ratios R_E , R_C and R_S .

208

209 In the absence of the source S (or taking $R_S = 1$), should one be interested in tagging the
 210 water that originates from some geographical location defined as those model grid points
 211 (X, Y) and time (T) , a useful choice is $R_C = q_i/q$, and an evaporative source mask can be
 212 defined such that

$$213 \quad R_E = \begin{cases} 1 & \forall (x, y, t) \in (X, Y, T) \\ 0 & \text{otherwise} \end{cases}. \quad (\text{X.3})$$

214 Fig 1 shows a case where the region of interest is defined as southern South America, and
 215 the quantity plotted is the fraction of total precipitation that results from
 216 evapotranspiration in that region. Values over the region itself give the recycling rate
 217 (i.e., the fraction of rain which came from local evapotranspiration). Values are high
 218 downstream and to the west in the southern midlatitudes and near the equator to the east

219 where the source water is entrained into the tropical easterlies. The source in this case
220 was defined without a time constraint, but the methodology can be adapted to track water
221 from, say, a given month. More elaborate source mask functions of $R_E = f(x, y, t)$ that are
222 smooth have some numerical advantages because numerical transport of step-like
223 anomalies is almost always problematic. Rather than considering surface sources, one can
224 tag other water sources, such as the evaporation of ice crystals, water of stratosphere
225 origin, water that has experience super-saturation, or any other specific condition that is
226 of interest.

227

228 The tagging methodology is a required first step in building an isotope scheme, and
229 indeed developing the code infrastructure to correctly tag the water, generate appropriate
230 flux statistics comparable to, say, precipitation and evaporation, and handle archiving of
231 model results, accounts for most of the effort in building an isotope scheme in
232 comprehensive models. This is unlike the simpler task of tagging air masses, since the
233 partitioning of water tracers changes during each instance of existing hydrological
234 exchange. That is, one must account for the known (calculated) terms E , C and S in a
235 hydrologic tracer scheme, while these are not present in gas-phase tracer schemes in
236 which only transport is needed.

237

238 The difference between a tagging scheme and an isotope scheme is simply that the ratios
239 R_E , R_C and R_S are modified by physically based fractionation, and i is a particular
240 isotopologue rather than a generic tracer. In practice one can have a tagged-isotope
241 scheme such that that isotopic composition of water from some specified source is

242 tracked (e.g., Noone and Simmonds 2002b). Fig 1b shows the $\delta^{18}\text{O}$ of the water that
243 originated from South America in a climate simulation. Notice the depletion away from
244 the source region, and that the resulting pattern in some ways resembles the rainout that
245 one expects from Rayleigh distillation. In this case, however, the distillation is combined
246 with large-scale and turbulent mixing processes which ensures the simulation result is
247 strictly (and quantifiably) non-Rayleigh. Such results provide significant diagnostic
248 capabilities for understanding the final isotope distributions beyond simple attribution to
249 different origins.

250

251 ***X.3.2 Numerical issues for transport processes***

252 Even though there is no fractionation associated with large-scale advection or during
253 (dry) turbulent exchange, some care is needed in a numerical implementation. Because
254 water vapor abundance changes by at least four orders of magnitude in nature, any
255 numerical scheme must be able to resolve this range, plus three more orders of magnitude
256 if one is interested in deviations there order of 1 ‰. This is a significant numerical
257 challenge. Jouzel et al. (1987) found that the advection scheme used in the GISS model
258 of the time was unable to conserve isotope ratios which introduced an isotopic
259 fractionation. Artificial fractionation during transport is a purely numerical issue, but is
260 clearly non-trivial and persists even in recent isotope schemes (Yoshimura et al. 2008).
261 Noone and Simmonds (2002b) found that the treatment of water vapor transport via
262 spectral methods was inadequate to preserved the isotope ratio in very low temperature
263 regions such as Antarctic and the upper troposphere, and lead them to replace their
264 spectral advection scheme with the semi-Lagrangian scheme of Williamson and Rasch

265 (1989). The spectral method, while appealing for resolving sharp gradients in dynamic
266 fields (i.e., cold fronts), is remarkably poor at conserving covariance between two tracers
267 (such as H₂O and any other isotopologue) in the region of such gradients. While the semi-
268 Lagrangian scheme better preserves tracer-tracer correlations, it is not conservative, and
269 the addition of mass fixers to ensure global conservation introduces a non-physical
270 component to the transport. This is usually small compared to the dominant physical
271 signal, at least in the lower troposphere where the lifetime of water is reasonably short.
272 Prather et al. (1986) developed a highly accurate numerical scheme based on the
273 describing the sub-grid scale structure with quadratic moments, and which has been
274 found to preserve isotope ratios adequately in the GISS model (Schmidt et al. 2005). A
275 numerical scheme that is expressly designed to preserve tracer-tracer correlations was
276 developed by Lin and Rood (1996) and guarantees the isotope ratio R will be preserved
277 under advection of q and q_i independently. However, in all cases, more complicated
278 schemes require more numerical operations and faster computers, and thus the ultimate
279 choice is a practical compromise.

280

281 Part of the result stems from the choice of the state variable. The most physically
282 meaningful choice is the isotope mass mixing ratio (or number density), such that the
283 isotope budget perfectly mirrors the underlying water cycle given by (X.1), but another
284 choice is the isotope ratio itself. Transforming (X.1) into a budget equation for the ratio R
285 is straightforward, and given R and q , the source and sink terms can still be included as
286 influences on q_i as needed. One can obtain the numerical benefits of using R in transport,

287 by writing the isotope mass flux as the sum of a “base state” component, plus an “isotope
 288 flux” by appealing to the product rule:

$$289 \quad \mathbf{V} \cdot \nabla q_i = R(\mathbf{V} \cdot \nabla q) + q(\mathbf{V} \cdot \nabla R). \quad (\text{X.4})$$

290

291 While algebraically the same, the small differences that project onto numerical
 292 uncertainties provide substantial differences in the resulting δ values². Jouzel et al. (1987)
 293 found a solution to the transport problem in the GISS model by using a scheme like
 294 (X.4), and considered the isotope advection relative to the advection of water.

295 Improvements from such an approach are greatest for the least accurate schemes, and
 296 indeed the advantage in the Lin and Rood’s (1996) finite-volume scheme is trivial.

297 Treatment of non-resolved fluxes by diffusion is subject to similar artifacts (particularly
 298 in boundary layer schemes that parameterize “non-local” transport), and these also can be
 299 overcome by recognizing no numerical scheme is perfect and designing a scheme in
 300 which the numerical precision is better than that needed for a given magnitude physical
 301 signal is the main requirement. The precision needed for isotopes is three orders of

² Consider the inequality that results from simplest one-dimensional centered finite difference approximation to (X.4):

$$\frac{u}{2\Delta x} (q_i^+ - q_i^-) \neq \frac{u}{2\Delta x} \left[\frac{q_i}{q} (q^+ - q^-) + q \left(\frac{q_i^+}{q^+} - \frac{q_i^-}{q^-} \right) \right]$$

where the subscripts + and – denote values evaluated as some position $x+\Delta x$ and $x-\Delta x$, and values without subscripts are evaluated at position x . The error that leads to the inequality is a result of the order of the finite approximation, and the size of the error can be as large as the isotope variations of interest in cases where the changes in q are large relative to q .

302 magnitude greater than for non-isotope applications because the physical signal of
303 interest is measured in units of per mil.

304

305 **X.4 Exchange processes and fractionation**

306 *X.4.1 Land and ocean water sources*

307 Craig and Gordon (1965) suggested a model for the evaporative flux of isotopes from
308 both open water and through vegetation. These ideas persist to today and are considered
309 both robust and applicable for modeling isotopic exchange in many instances. They posit
310 that, following a Fickian transport process, one can express evaporation as a flux
311 associated with mixing between ambient air and a reservoir of vapor that is in
312 thermodynamic equilibrium with open water (say, ocean). This is a special case of a more
313 general description of water mass mixing (Noone 2009). As such, the evaporative flux
314 can be written:

$$\begin{aligned} E &= \rho c (q_s - q) \\ E_i &= \rho \eta c (R_s q_s - q_i) \end{aligned} \tag{X.5}$$

316 where c is an exchange coefficient (or, conductance), q_s is the saturation mixing ratio at
317 the source temperature T_s , and ρ is the density of dry air. The two terms E and E_i can
318 immediately be combined to give an expression for the isotope ratio of the flux R_E .

319

320 The isotopic flux E_i , depends on the isotopic composition of the source vapor R_s . Over
321 the ocean this can be taken as $R_s = R_{ocean}/\alpha_e$, where α_e is the equilibrium fractionation
322 factor which depends on the surface temperature (T_s). Fig 2a shows the annual mean $\delta^{18}\text{O}$

323 of precipitation simulated by a model in which only the surface fluxes fractionate (no
324 fractionation is applied during condensation). Noone (2009) demonstrated that a mixing
325 processes, such as evaporation and evapotranspiration, tends toward a steady state value
326 set as the weighted mean of all source waters, which in this case is dominated by the
327 infinite ocean source. As such the vapor tends toward the flux-weighted mean value of
328 vapor in equilibrium with the ocean. Notice that the equilibrium fractionation factor is
329 weakly temperature dependant over the range 0-35°C that spans the global SST
330 distribution, and gives rise to the spatial variation seen in the figure. Given the global
331 mass weighted mean value of precipitation from this simulation of $\delta^{18}\text{O} = -10.05 \text{‰}$, one
332 finds the mean temperature of evaporation is 289 K, which corresponds with ocean
333 surface temperature in the region of the extratropics and mid-latitudes. The rate at which
334 the model approaches this steady state value is a function of the surface exchange
335 coefficient (c), the kinetic fractionation efficiency (η), the strength of turbulence in the
336 boundary layer, and large scale mixing by small and large-scale motions, and is on the
337 order of months.

338

339 At steady state, Craig and Gordon (1965) showed that the isotopic composition of the
340 water flux from plants must equal the isotopic composition of the soil water (Helliker and
341 Noone , this volume), and so $R_s=R_{soil}$ and there is no apparent fractionation. Dongmann et
342 al. (1974) relaxed the steady state assumption and showed that Craig and Gordon's
343 simpler model is often quite satisfactory in the time-mean. A non-steady state assumption
344 has subsequently been used in a sophisticated process model by Noone et al. (2002) and
345 Still et al. (2009), who again find for long-term statistics the steady-state assumption is

346 quite valid, and only when one is interested in variations on, say, diurnal time-scales does
347 one need to account for non-steady conditions.

348

349 The factor η in (X.5) accounts for the slightly differing conductance of isotopologues
350 compared to normal water, and is slightly less than one. This arises because the total flux
351 is composed of both transport by molecular diffusion and by turbulent eddy motions.

352 While the transport by turbulence has no fractionation, the diffusive component for the
353 different isotopologues introduces kinetic fractionation. Merlivat and Jouzel (1979)
354 studied the influence of this kinetic effect as a function of the turbulent strength, and
355 showed a clear transition as a function of the Richardson number (and thus, friction
356 velocity), or near-surface wind speed (η here is equivalent to their $1-k_{\text{mol}}$). Their
357 parameterized theory is in common use for oceanic fluxes in global models, although
358 there remains some question as to the value of some parameters (Cappa et al. 2003).

359

360 An alternate, but equivalent, approach was taken by Riley et al. (2002), who explicitly
361 wrote down the isotopic conductances associated with both turbulent and diffusive fluxes
362 in the case of transpiration and evaporation from soils. The advantage of Riley's scheme
363 stems from the knowledge of both the molecular and turbulent components in the
364 underlying model (Bonan 1994; Bonan et al. 1997). That is, the physics that controls the
365 isotopic kinetic effect are represented explicitly. Because the fractionation is tied more
366 directly to the model physics this is a more satisfying approach than introducing an
367 additional parameterization.

368

369 ***X.4.2 Elementary cloud processes in comprehensive models***

370 Within a modeled hydrologic cycle condensation and evaporation is parameterized
371 depending on a number of large scale variables, including temperature and humidity. The
372 humidity of an air mass changes due to variation in the moisture and temperature fields
373 because of any number of the dynamic or thermodynamic influences simulated, and
374 condensation can occur when vapor reaches some fraction of the saturation value. If the
375 condensation is slow, then it can be considered thermodynamically reversible (as in a
376 reversible moist adiabatic process, Noone 2009), and one can assume the formation of
377 cloud liquid droplets occurs at isotopic equilibrium (i.e., a closed system). On the other
378 hand if condensation is fast, to larger drops or the condensate is ice, the molecules
379 composing the hydrometeors are effectively separated from the vapor and an open-
380 system (Rayleigh) assumption is more reasonable. The first implementations of isotope
381 tracers in a global models used this physical reasoning to model isotopic fractionation
382 that accompanies rain formation by stratiform cloud as an open process, and formation of
383 ice condensate and either ice or liquid condensate from convective cloud as a Rayleigh
384 process. We will refer here to isotope schemes of this type as “first generation” isotope
385 schemes for the treatment of cloud processes. While the concepts are borrowed from
386 simpler box/trajectory models, such a fractionation scheme can be fitted to
387 comprehensive dynamical models.

388

389 The use of close-system assumption in a discrete spatial model provides a finite estimate
390 of the (continuous) Rayleigh process, and as such, any model that uses this assumption
391 will ultimately represent a distribution that approximates a Raleigh distillation. On the

392 other hand, the choice of using a Rayleigh processes to model convective condensation is
 393 akin to suggesting a time-scale separation between the processes which operate within
 394 clouds and those associated with the large-scale flow, and is an assumption that is
 395 implicit to all large scale models that do not track the evolution of cloud liquid and ice.
 396 Indeed prognosis of cloud liquid is required in high resolution models to explicitly
 397 account for sub-Rayleigh behavior if there is cloud liquid retained. This has been
 398 demonstrated analytically by Noone (2009) for the case of the two-phase model given by
 399 Merlivat and Jouzel (1984). On the other hand, the correct sub-Rayleigh behavior is
 400 implicit in low resolution dynamical models as a resolution artifact.

401

402 Given these considerations, one can envisage the simplest (but still comprehensive)
 403 isotope model in which one has an H₂O tracer, along with HDO and H₂¹⁸O tracers. There
 404 is some surface source, say given by (X.5), and the resulting water is subject to transport
 405 by non-fractionating large-scale motion, turbulent boundary layer motion, and by
 406 convective updrafts and downdrafts. A check is made at each time step for each grid box
 407 to see if the tracer water has exceeded saturation at the environmental temperature. If so,
 408 an adjustment (Δq_i) is made as either an open or closed isotope exchange such that

$$\begin{aligned}
 &\Delta q = \min(h_c q_s(T) - q, 0) \leq 0 \\
 409 \quad \Delta q_i = &\begin{cases} q_i \left[\frac{1}{\alpha(1-F^{-1})} - 1 \right]^{-1} & T > T_{freeze} \text{ and small drops} \cdot \\ q_i (F^\alpha - 1) & T < T_{freeze} \text{ or large drops} \end{cases} \quad (X.6)
 \end{aligned}$$

410 The fraction of vapor remaining after the adjustment (final/initial), F , is given by

$$411 \quad F = \frac{h_c q_s}{q} = 1 + \frac{\Delta q}{q} \leq 1 \quad (X.7)$$

412 where h_c is some critical relative humidity (often taken as 80% for a grid-cell mean), and
413 the freezing temperature, T_{freeze} , could be taken below 0°C where super-cooled liquid
414 exists. In practice some care is needed to ensure solution of (X.6) avoids divide by zero
415 errors when F becomes small. Choice of the fractionation factor as the equilibrium value
416 when condensation is to liquid is robust since this is assumed a slow process. During
417 formation of ice condensate, the diffusivity slows the transport of vapor onto growing ice
418 crystals, and this limitation is greater for the heavier isotopologues. Specifically, while
419 there is a preference for the heavy nuclides to condense, the strength of this preference is
420 reduced through the kinetic limitation. Jouzel and Merlivat (1984) introduced a
421 parameterization for the kinetic effect as a function of supersaturation of the vapor in the
422 presence of ice, which remains in common use in isotope models.

423

424 Fig 2b shows a model simulation for the case where fractionation during condensation is
425 applied only during stratiform condensation as by (X.6). Notice that in the tropics the
426 influence enriches the precipitation relative to the original vapor because the
427 condensation temperature is lower than the (surface) evaporation temperature and thus
428 fractionation is more efficient. The removal of heavy isotopes at midlatitudes gives rise to
429 the latitude effect, as seen in the greater depletion at higher latitudes and particularly over
430 Antarctica and Greenland. Indeed, with fractionation in only stratiform cloud there is
431 evidence for the latitude, altitude and continental effects noted by Dansgaard (1964). The
432 impact of fractionation associated with convection is seen in Fig 2c to mainly influence
433 the spatial structure in the tropics and over land, where a large fraction of the total
434 precipitation is associated with convective storms. At high latitudes a depleting influence

435 is again seen because of condensation upstream, with subsequent transport of the
436 remaining depleted vapor toward the poles. Indeed the globally integrated influences of
437 fractionation during condensation is small (+0.66 ‰ for stratiform, and +0.18 ‰ for
438 convective), and non-zero only because of non-linearity introduced by transport. As such,
439 the importance of fractionation during condensation is best seen as affecting the spatial
440 distribution, while the strength of fractionation associated with the surface fluxes, sets the
441 mean. Notice that combining these two condensation terms, a spatial pattern emerges that
442 is consistent with a spatial view of Dansgaard's empirical amount effect since the tropical
443 regions where precipitation totals are higher are more depleted than the higher
444 (subtropical) latitudes.

445

446 *X.4.3 More advanced isotope cloud physics*

447 First generation cloud schemes need not be tied all that closely to the underlying physical
448 model yet can provide satisfying results for many applications. A second generation
449 cloud isotope scheme incorporates more explicit treatment of hydrological exchanges
450 within convective clouds, rather than simply applying a single bulk fractionation to
451 capture the entire behavior of the cloud. Specifically, modern atmospheric GCMs
452 represent the transport with the region of convection via convective updrafts and
453 downdrafts. As indicated in Table 1, most isotope models presently in use can be
454 described as of this type since they account in some way for convective scale transport.
455 Accounting for fractionation within clouds is more complicated, but there are some
456 simple bulk assumptions about isotopic exchange that can be made. For instance, in
457 updrafts, rapid condensation ensures the environment is near-saturated with respect to the

458 in-cloud temperature giving motivation for a Rayleigh distillation. Similarly, the
 459 existence of downdrafts is associated with evaporation of rain, and one might assume that
 460 these regions are also (near) saturated, and so isotopically close to equilibrium with liquid
 461 drops.

462

463 Within a region of convective clouds one can write the tendency associated with
 464 convection as

$$465 \quad \left(\frac{\partial q}{\partial t} \right)_{convective} = \frac{\partial(w'q')}{\partial p} \approx \frac{\partial}{\partial p} [w_u (q - q_u)] \quad (\text{X.8})$$

466 where the subscript u indicates quantities in the updraft region, and an elementary mass
 467 balance for the in-cloud vapor can be written as

$$468 \quad \frac{\partial q_u}{\partial t} = \frac{\partial(mq_u)}{\partial p} - C + \gamma - \mu q_u = 0. \quad (\text{X.9})$$

469 The budget equation of updraft water is assumed at steady state, which is justified by
 470 noting the timescale separation between convection (less than an hour) and the resolved
 471 large-scale motion (order of a day). The rate at which water vapor from outside the
 472 plume is entrained is γ , μ is the rate of detrainment of the plume material, and m is the
 473 vertical mass flux. The mass flux is related to the updraft velocity ω_u through knowing
 474 the fraction of the grid box covered by updrafts. From conservation considerations, m , γ
 475 and μ are related (consider the case with $C=0$ and $q_u=q=1$). An isotopic version of (X.8)
 476 follows by assuming the vertical profile in q_u satisfies a Rayleigh profile, and so isotopic
 477 composition of condensation is set via equilibrium with the vapor (with a kinetic effect if
 478 the condensation is to ice). Because the convective mass flux, m , is found as part of the
 479 underlying convective parameterization, this is a reasonably convenient form. This

480 approach can easily be adapted for models that track cloud liquid and ice in addition to
481 large-scale vapor. Similarly, an expression analogous to (X.9) but for downdrafts can be
482 written upon assuming that downdrafts are saturated, and one writes the isotopic
483 composition of the downdraft as that in (or close to) equilibrium with precipitation falling
484 in the downdraft region if liquid or resulting from non-fractionating sublimation if the
485 precipitation is frozen.

486

487 Such second generation schemes begin to address issues surrounding the isotopic
488 partitioning in the region of clouds. While this added complexity may not have a
489 substantial influence on the simulated isotopic composition of precipitation, the
490 microphysical and isotopic assumptions greatly influence the simulation of the isotopic
491 composition of mid and upper troposphere water vapor. Schemes of even this complexity
492 are not easily employed in models simpler than comprehensive dynamical models.

493

494 Third generation cloud isotope schemes are beginning to appear and represent the state of
495 the art. They differ in their design by specifically fitting isotope physics to the more
496 detailed cloud processes within modern atmospheric models. This is motivated in part by
497 a desire to understand the isotopic exchange within clouds, rather than the isotopic
498 composition that results from clouds in some average sense. To this end, the development
499 of third generation models is facilitated by more detailed bulk microphysical schemes
500 being used in modern climate and Earth-system models. Fig 3 shows a schematic
501 example of a third-generation isotope cloud model and depicts the multiple exchanges
502 between different microphysical moments that are explicitly (or implicitly) accounted for

503 in the underlying non-isotopic cloud model. This scheme treats both grid-average and in-
504 cloud vapor, cloud liquid, cloud ice, liquid drops (rain) and ice precipitation (a
505 combination of snow, grauple and hail). Transport processes include the mixing between
506 grid-scale and in-cloud properties via entrainment and detrainment, and updraft and
507 downdraft fluxes as expressed in (X.8). Such models share some similarities with the
508 cloud models of Federer et al. (1982), Gedzelman and Arnold (1994), Lawrence et al.
509 (1998), Bony and Risi (2008), and the mixed-phase cloud model of Ciais and Jouzel
510 (1994). The computational demand of third-generation scheme is much greater since the
511 isotopic (bulk) microphysics needs to be solved via numerical integration over each
512 dynamical model time step to be accurate, which contrasts with second-generation
513 schemes in which the bulk exchanges can be directly computed via integral expressions
514 of the required adjustment, as, for instance, given by (X.6). It is this numerical
515 requirement and the complexity of web of exchanges within clouds that separates second
516 and third generation schemes.

517

518 Fourth generation cloud isotope schemes can be foreseen as those in which the
519 microphysical exchanges (such as diffusional particle growth and coalescence processes)
520 are resolved and isotopic exchanges can be computed directly, rather than resorting to the
521 bulk microphysics used in third generation schemes. An example of a such as scheme
522 was used at cloud resolving scales with a detailed microphysical scheme by Smith et al.
523 (2006). Such schemes will place constraints on the underlying assumed microphysics,
524 which themselves are not well known, since both equilibrium and kinetic isotopic
525 exchanges are resolved as first principles processes rather derived from assumptions

526 surrounding bulk microphysics. The practical issue of applying explicit microphysical
527 schemes in large-scale models remains a challenge for the non-isotopic modeling
528 community, and is an area where isotope constraints are may be particularly informative.
529

530 *X.4.4 Post condensation exchange*

531 Although the cloud processes control the primary removal of water from the free
532 atmosphere, Jouzel (1986) noted that the time taken for liquid drops to equilibrate with
533 the environment through which they fall is usually comparable, and often shorter than,
534 the time required to reach equilibrium. The effect results from two drop-size dependant
535 features: 1) small drops fall slowly, and 2) small drops equilibrate quickly. As such,
536 sufficiently small rain drops will equilibrate with vapor near the ground, and the isotopic
537 composition of liquid precipitation will closely resemble the isotopic composition of near
538 surface (boundary layer) vapor. Stewart (1975) noticed this effect and explained the
539 tendency toward the equilibrium as a mixing process.

540

541 The exchange mechanism has been used to explain the amount effect that Dansgaard
542 observed (Stewart 1975; Rozanski et al. 1993; Worden et al. 2007; Bony and Risi 2008;
543 Lee and Fung 2008; Noone 2009). Because the sub-cloud layer is sub-saturated (by
544 definition), isotopic exchange is usually accompanied by a net evaporation of the falling
545 rain, and exchange provides a net recycling of molecules between the condensate and the
546 free atmospheric vapor (Worden et al. 2007; Noone 2009). In this way, the isotopic
547 composition provides a metric of the efficiency with which water is removed from the
548 atmosphere as precipitation.

549

550 While the solid matrix of ice precipitation prohibits any equilibration, large rain drops
551 associated heavy rain events will undergo partial equilibration. Hoffmann et al. (1998)
552 suggested that in a comprehensive model rain under convective clouds experiences 45%
553 equilibration, while stratiform cloud (with assumed smaller drops and lower rainfall
554 rates) almost completely equilibrate (95% equilibration). Lee et al. (2008) used a
555 parameterization of the drop size distribution to allow this rate to be calculated within the
556 model based on the modeled precipitation rates. Fig 2d shows the impact of allowing
557 isotopic equilibration using a similar physically based scheme on the final precipitation.
558 Notice that at high latitudes where the precipitation is largely ice, and in the tropics where
559 the raindrops are typically large and associated with convection, the partial equilibration
560 has limited influence. Generally the influence is to enrich the precipitation (the globally
561 integrated enrichment is +1.45 ‰) and is largest in the subtropical regions where the sub-
562 cloud relative humidity is low. With enriched precipitation the remaining tropospheric
563 vapor is consequently more depleted. The depleting influence at high latitudes thus
564 results from transport of vapor that has undergone this depleting influence at lower
565 latitudes.

566

567 The isotopic composition of all but the heaviest rain is set through isotopic exchange as it
568 falls from clouds, and because the vapor near the surface ocean is tied to ocean water via
569 the exchange coefficient c in (X.5), only in regions that are far from equilibrium, should
570 the precipitation deviate much from that set by exchange at the ocean surface. It is for
571 this reason that atmospheric models, in which the strength exchange process can be

572 tuned, can simulate the isotopic composition of precipitation over the ocean and moist
573 continental regions with high fidelity. Doing so, however, does not suggest that these
574 models accurately simulate the atmospheric hydrology and clouds processes in detail.
575

576 **X.5 Interpretive utility and reproducibility**

577 All models can be used with either the goal of reproducing some set of data, or being
578 used to test the importance of some specific physics or processes being modeled.
579 Illustrating the case of reproduction, Fig 4 shows the annual mean $\delta^{18}\text{O}$ composition in
580 precipitation from the three global isotope models that participated in the first Stable
581 Water-isotope Intercomparison Group (SWING) experiment, compared to the
582 observationally based map of Buening and Noone (2008). It shows that many of the
583 spatial features are reproduced, including the dominant latitude, altitude, continental and
584 amount effects. However, there are also substantial model errors. While the three models
585 all fit GNIP-based map with a root mean squared error around 2 ‰, errors the order of 2
586 ‰ can often be too large for applications. Closer examination of Fig 4 reveals that many
587 of the regions with largest model error are associated with regions where the underlying
588 hydrology is less robust, and tied to deficiencies in the simulation of large scale transport,
589 problems with cloud physics and poor representation of surface hydrology.

590

591 The deuterium excess simulation (Fig 5) is even more problematic because the less
592 precise knowledge of kinetic effects. Similarly, many of the environmental conditions
593 that give rise to kinetic effects are not modeled by the underlying hydrologic scheme
594 (such as supersaturation, or the partitioning of molecular and turbulent transport during

595 evaporation), and thus ultimately not well accounted for. To this end, mapping isotope
596 distributions with comprehensive models is ultimately limited by both the robustness of
597 the underlying model hydrology and the strength of the assumptions about the isotopic
598 physics. Because the isotope physics in all but fourth generation schemes use bulk
599 microphysical implementations of the isotope exchange, there is some uncertainty in the
600 degree to which any errors in the final isotope fields is associated with the isotope
601 scheme versus other errors in the underlying hydrological or climate simulation. Usually,
602 isotope studies attribute much of the error to the underlying model with the assumption
603 that the uncertainty in the isotope physics is much smaller than other model problems, but
604 this has never been well quantified.

605

606 **X.6 Discussion and outlook**

607 While the advantages of comprehensive models are substantial, they are of course subject
608 to a different set of limitations experienced by simpler models. Specifically, the
609 simulation quality reflects both the detail to which the contributing processes are
610 understood and the accuracy with which those processes are represented numerically. In
611 part because of computational demand, no single aspect of these comprehensive models
612 (clouds, land surface exchange, transport, etc.) is the most detailed available. This
613 naturally places limits on the type of science questions that can be explored with such
614 models. On the other hand, models of any complexity can be configured to provide
615 meaningful results for some science application, and the choice to use comprehensive
616 dynamical models of isotopes must stem from a need to account for combinations of
617 processes or variability not well captured by simpler models. While the maps that result

618 from comprehensive dynamical isotope models are useful in their own right for follow-on
619 studies, a valuable use of isotopic models is in diagnosing the behavior of various
620 processes. Indeed the most powerful use of these models is in the ability to probe the
621 mechanisms responsible for the true isotope distributions.

622

623 Being based on some underlying dynamical model, any biases in simulated climate
624 variables (temperature, boundary layer dynamics, etc.) are reflected in the simulated
625 isotopic distribution. The agreement between observations and simulations increases
626 when some aspects of the simulation can be constrained. Recent interest has arisen in
627 using isotopic models in which the large-scale meteorology is prescribed (say, nudged,
628 Noone 2006; Yoshimura et al. 2008) and it is found that the simulated isotopic variability
629 is remarkably robust on both daily and longer time scales. While this is a reminder that
630 many aspects of the isotopic variability are associated with the large-scale transport
631 pathways, it also suggest that constrained simulations are helpful in understanding the
632 impact of synoptic circulation variability and organized patterns of variability (e.g., El
633 Niño Southern Oscillation or North Atlantic Oscillation) on some observed isotopic
634 record.

635

636 Comprehensive models lend themselves to hypothesis testing via sensitivity tests which
637 can inform as to which types of mechanisms one should expect to influence a given set of
638 measurements. This capability is at least of equal importance as the ability of
639 comprehensive models to reproduce known isotopic distributions. While global scale
640 models are especially useful in providing climatological understanding of isotope

641 distributions, they are often not able to match isotope observed distributions because of
642 the need to use relatively coarse resolution. This is of particular concern when the
643 isotopic composition depends on geographic structures (topography, vegetation
644 classification, coastlines) which are not well captured by relatively low resolution global
645 models. Increasing the spatial resolution has several advantages, but it comes at a high
646 cost in terms of computational burden. One option is therefore to use regional circulation
647 models (RCM) for high resolution isotope studies over some region of interest (Sturm et
648 al. 2005; Sturm et al. 2007a). While the gap between the resolution of RCMs and global
649 models has narrowed, many regional models now can be configured to run just short of
650 resolving individual clouds and have other benefits.

651

652 Simulating isotopes within comprehensive dynamical models is a task which is limited by
653 appropriate datasets for validation and testing. The International Atomic Energy
654 Agency's GNIP remains a gold standard for testing global and regional models, but as
655 argued here, these data do not provide a rigorous test of isotopic exchanges associated
656 with cloud processes. Indeed even if the precipitation isotopes are simulated accurately, it
657 is not a guarantee that the atmospheric water vapor isotopes are also simulated reliably
658 because of post condensation exchange. Very few observations of the isotopic
659 composition of water vapor exist, yet since this is the state variable in isotope models (as
660 compared to the precipitation, which is a by-product flux), direct evaluation of the vapor
661 phase is highly desirable. Complimenting traditional water vapor collection and analysis
662 methods, new observational techniques (including in situ and satellite based observations,
663 Helliker and Noone, this volume) are poised to allow more detailed testing of specific

664 isotope physics and hydrologic balances within comprehensive models, and will likely
665 foster significant model improvements. The need for increased rigor in validation is
666 particularly warranted as the scope of scientific investigations to which comprehensive
667 isotope models are being applied expands. Similarly, with greater validation effort comes
668 increased confidence in the spatially and temporally resolved isotopic distributions that
669 are simulated, and thus increased capacity to use the outputs from comprehensive
670 dynamical isotope models as input to subsequent applications and isoscaping.

671

672 **References**

- 673 Bonan GB (1994) Comparison of 2 Land-Surface Process Models Using Prescribed
674 Forcings. *Journal of Geophysical Research-Atmospheres* 99:25803-25818
- 675 Bonan GB, Davis KJ, Baldocchi D, Fitzjarrald D, Neumann H (1997) Comparison of the
676 NCAR LSM1 land surface model with BOREAS aspen and jack pine tower
677 fluxes. *Journal of Geophysical Research-Atmospheres* 102:29065-29075
- 678 Bony S, Risi C (2008) Influence of Convective Processes on the Isotopic Composition
679 (d18O and dD) of Precipitation and Water Vapor in the Tropics: 1. Radiative-
680 Convective Equilibrium and TOGA-COARE Simulations. *Journal of Geophysical*
681 *Research in review*, April 2008
- 682 Bosilovich MG, Schubert SD (2002) Water vapor tracers as diagnostics of the regional
683 hydrologic cycle. *Journal of Hydrometeorology* 3:149-165
- 684 Brown J, Simmonds I, Noone D (2006) Modeling delta O-18 in tropical precipitation and
685 the surface ocean for present-day climate. *Journal of Geophysical Research-*
686 *Atmospheres* 111, D05105, doi:10.1029/2004JD005611
- 687 Buenning N, Noone D (2008) The role of local and non-local processes in the seasonal
688 cycle and interannual variability of the isotopic composition of precipitation
689 deduced through observations and models. *Journal of Geophysical Research in*
690 *review*, June 2008
- 691 Cappa CD, Hendricks MB, DePaolo DJ, Cohen RC (2003) Isotopic fractionation of water
692 during evaporation. *Journal of Geophysical Research-Atmospheres* 108:4525,
693 doi:4510.1029/2003JD003597

694 Charles CD, Rind D, Healy R, Webb R (2001) Tropical cooling and the isotopic
695 composition of precipitation in general circulation model simulations of the ice
696 age climate. *Climate Dynamics* 17:489-502

697 Ciais P, Jouzel J (1994) Deuterium and oxygen 18 in precipitation: an isotopic model
698 including mixed cloud processes. *J. Geophys. Res.* 99:19783-16803

699 Cole JE, Rind D, Webb RS, Jouzel J, Healy R (1999) Climatic controls on interannual
700 variability of precipitation $\delta^{18}\text{O}$: simulated influence of temperature, precipitation
701 amount, and vapor source region. *J. Geophys. Res.* 104:14223-14235

702 Craig H, Gordon LI (1965) Deuterium and oxygen-18 variations in the Ocean and Marine
703 Atmosphere. In: Tongiorgi E (ed) *Proceedings of Conference on Stable Isotopes
704 in Oceanic Studies and Paleotemperatures. Lab. Geol. and Nuclear Sci., Spoleto,
705 Italy, pp 9-130*

706 Dansgaard W (1964) Stable isotopes in precipitation. *Tellus* 16:436-468

707 Dongmann G, Nürnberg HW, Förstel H, Wagener K (1974) On the enrichment of H_2^{18}O
708 in the leaves of transpiring plants,. *Radiation and Environmental Biophysics* 11:41-
709 52

710 Federer B, Brichet N, Jouzel J (1982) Stable isotopes in hailstones, I, the isotopic cloud
711 model. *J. Atmos. Sci.* 39:1323-1336

712 Gedzelman SD, Arnold R (1994) Modeling the isotopic composition of precipitation. *J.*
713 *Geophys. Res.* 99:10455-10471

714 Helliker B, Noone D (2009) Novel approaches to monitoring of water vapor isotope
715 ratios: Plants, satellites and lasers. In: West J, Bowen G, Dawson T, Tu K (eds)

716 Isoscapes: Understanding movement, pattern, and process on Earth through
717 isotope mapping. Springer

718 Hoffmann G (1995) Wasserisotope im allgemeinen Zirkulationsmodell ECHAM. In.
719 Universitat Hamburg, Hamburg

720 Hoffmann G, Heimann M (1997) Water isotope modeling in the Asian monsoon region.
721 Quart. Int. 37:115-128

722 Hoffmann G, Jouzel J, Masson V (2000) Stable water isotopes in atmospheric general
723 circulation models. Hydrol. Process. 14:1385-1406

724 Hoffmann G, Werner M, Heimann M (1998) Water isotope module of the ECHAM
725 atmospheric general circulation model: A study on timescales from days to
726 several years. J. Geophys. Res. 103:16871-16896

727 Joussaume S (1983) Modélisation des cycles des espèces isotopiques de l'eau et des
728 aerosols d'origine de'ésertique dans un modele de circulation generale de
729 l'atmosphere. In. Univeristy of Paris, Paris, France

730 Joussaume S (1993) Paleoclimate tracers: An investigation using an atmospheric general
731 circulation model and ice age conditions 1. Desert dust. J. Geophys. Res.
732 98:2767-2805

733 Joussaume S, Jouzel J (1993) Paleoclimatic tracers: an investigation using an atmospheric
734 general circulation model under ice age conditions. 2. Water isotopes. J. Geophys.
735 Res. 98:2807-2830

736 Joussaume S, Jouzel J, Sadourny R (1984) A general circulation model of water isotope
737 cycles in the atmosphere. Nature 311:24-29

738 Jouzel J (1986) Isotopes in cloud physics: multistep and multistage processes. In: Fritz P,
739 Frontes JC (eds) Handbook of environmental isotope geochemistry, vol.2, The
740 terrestrial environment B. Elsevier, New York, pp 61-112

741 Jouzel J, Koster RD, Suozzo RJ, Russel GL, White JW, Broecker WS (1991) Simulations
742 of the HDO and H₂¹⁸O atmospheric cycles using the NASA GISS general
743 circulation model: sensitivity experiments for present day conditions. J. Geophys.
744 Res. 96:7495-7507

745 Jouzel J, Merlivat L (1984) Deuterium and oxygen 18 in precipitation, modelling of the
746 isotopic effects during snow formation. J. Geophys. Res. 89:11749-11757

747 Jouzel J, Russell GL, Suozzo RJ, Koster RF, White JWC, Broecker WS (1987)
748 Simulation of the HDO and H₂¹⁸O atmospheric cycles using the NASA GISS
749 general circulation model: the seasonal cycle for present-day conditions. J.
750 Geophys. Res. 92:14739-14760

751 Koster R, Jouzel J, Suozzo R, Russell G (1986) Global sources of local precipitation as
752 determined by the NASA/GISS GCM. Geophysical Research Letters 13:121-124

753 Koster RD, Valpine DPd, Jouzel J (1993) Continental water recycling and H₂¹⁸O
754 concentrations. Geophysical Research Letters 20:2215-2218

755 Lawrence JR, Gedzelman SD, Zhang X, Arnold R (1998) Stable isotope ratios of rain and
756 vapor in 1995 hurricanes. J. Geophys. Res. 103:11381-11400

757 Lee JE (2005) Atmospheric water: Perspectives from isotopes and the NCAR climate
758 model. In. University of California, Berkeley, p 162

759 Lee JE, Fung I (2008) "Amount effect" of water isotopes and quantitative analysis of
760 post-condensation processes. Hydrological Processes 22:1-8

761 Lee JE, Fung I, DePaolo DJ, Henning CC (2007) Analysis of the global distribution of
762 water isotopes using the NCAR atmospheric general circulation model. *Journal of*
763 *Geophysical Research-Atmospheres* 112:D16306,
764 doi:16310.11029/12006JD007657

765 Lin SJ, Rood RB (1996) Multidimensional flux-form semi-Lagrangian transport schemes.
766 *Monthly Weather Review* 124:2046-2070

767 Mathieu R, Pollard D, Cole JE, White JWC, Webb RS, Thompson SL (2002) Simulation
768 of stable water isotope variations by the GENESIS GCM for present-day
769 conditions. *J. Geophys. Res.* 107:doi:10.1029/2001JD900255

770 McCarthy MC et al. (2004) The hydrogen isotopic composition of water vapor entering
771 the stratosphere inferred from high-precision measurements of delta D-CH4 and
772 delta D-H-2. *Journal of Geophysical Research-Atmospheres* 109:D07304,
773 doi:07310.01029/02003JD004003

774 Merlivat L, Jouzel J (1979) Global climatic interpretation of the deuterium-oxygen-18
775 relationship for precipitation. *J. Geophys. Res.* 84:5029-5033

776 Noone D (2003) Water isotopes in CCSM for studying water cycles in the climate
777 system. In: Eighth Annual CCSM Workshop, Breckenridge, Colorado

778 Noone D (2006) Isotopic composition of water vapor modeled by constraining global
779 climate simulations with reanalyses. In. World Meteorological Organization,
780 Research Activities in Atmospheric and Oceanic Modelling, J. Cote (Ed.), pp 2-
781 37

782 Noone D (2009) An isotopic evaluation of the factors controlling low humidity air in the
783 troposphere. *Journal of Climate* in review, June, 2008.

784 Noone D, Simmonds I (2002a) Annular variations in moisture transport mechanisms and
785 the abundance of $\delta^{18}\text{O}$ in Antarctic snow. *Journal of Geophysical Research-*
786 *Atmospheres* 107:4742, doi:4710.1029/2002JD002262

787 Noone D, Simmonds I (2002b) Associations between delta O-18 of water and climate
788 parameters in a simulation of atmospheric circulation for 1979-95. *Journal of*
789 *Climate* 15:3150-3169

790 Noone D, Still C, Riley W (2002) A global biophysical model of ^{18}O in terrestrial water
791 and CO_2 fluxes. In. World Meteorological Organization, *Research Activities in*
792 *Atmospheric and Oceanic Modelling*, H. Ritchie, (Ed.), pp 4.19-14.20

793 Noone DC (2001) A physical assessment of variability and climate signals in Antarctic
794 precipitation and the stable water isotope record. In: School of Earth Sciences.
795 University of Melbourne, Parkville, Victoria, Australia, p 404

796 Prather M (1986) Numerical advection by conservation of second-order moments.
797 *Journal of Geophysical Research* 91:6671–6681

798 Riley WJ, Still CJ, Torn MS, Berry JA (2002) A mechanistic model of $(\text{H}_2\text{O})\text{-O-18}$ and
799 $(\text{CO}_2)\text{-O-18}$ fluxes between ecosystems and the atmosphere: Model description
800 and sensitivity analyses. *Global Biogeochemical Cycles* 16:1095,
801 doi:1010.1029/2002GB001878

802 Risi C, Bony S, Vimeux F (2008) Influence of convective processes on the isotopic
803 composition (d^{18}O and dD) of precipitation and atmospheric water in the Tropics.
804 Part 2: Physical interpretation of the amount effect. *Journal of Geophysical*
805 *Research* in review, April 2008

806 Rozanski K, Araguas-Araguas L, Gonfiantini R (1993) Isotopic patterns in modern global
807 precipitation. In: Swart PK, Lohmann KC, McKenzie J, Savin S (eds) Climate
808 Change in Continental Isotopic Records. Geophysical Monograph Series. No. 78,
809 American Geophysical Union, Washington, pp 1-63

810 Schmidt GA, Hoffmann G, Shindell DT, Hu Y (2005) Modelling atmospheric stable
811 water isotopes and the potential for constraining cloud processes and stratosphere-
812 troposphere water exchange. *J. Geophys. Res.* 110:D21314,
813 doi:21310.21029/22005JD005790

814 Schmidt GA, LeGrande AN, Hoffmann G (2007) Water isotope expressions of intrinsic
815 and forced variability in a coupled ocean-atmosphere model. *Journal of*
816 *Geophysical Research-Atmospheres* 112

817 Smith JA, Ackerman AS, Jensen EJ, Toon OB (2006) Role of deep convection in
818 establishing the isotopic composition of water vapor in the tropical transition
819 layer. *Geophysical Research Letters* 33:L06812,
820 doi:06810.01029/02005GL024078

821 Stewart MK (1975) Stable isotope fractionation due to evaporation and isotopic exchange
822 of falling waterdrops: Applications to atmospheric processes and evaporation of
823 lakes. *J. Geophys. Res.* 80:1133-1146

824 Still CJ et al. (2009) The influence of clouds and diffuse radiation on ecosystem-
825 atmosphere CO₂ and C¹⁸O exchange. *Journal of Geophysical Research-*
826 *Biogeosciences* In press

827 Sturm C, Hoffmann G, Langmann B (2007a) Simulation of the stable water isotopes in
828 precipitation over South America: Comparing regional to global circulation
829 models. *Journal of Climate* 20:3730-3750

830 Sturm C, Langmann B, Hoffmann G, Stichler W (2005) Stable water isotopes in
831 precipitation: a regional circulation modelling approach. *Hydrological Processes*,
832 19:doi: 10.1002/hyp5979

833 Sturm C, Vimeux F, Krinner G (2007b) Intraseasonal variability in South America
834 recorded in stable water isotopes. *Journal of Geophysical Research-Atmospheres*
835 112:D20118, doi:20110.21029/22006JD008298

836 Sturm K (2005) Regional modelling of the stable water isotope cycle. In. Université
837 Joseph Fourier, Grenoble

838 Vuille M et al. (2003) Modeling delta O-18 in precipitation over the tropical Americas: 2.
839 Simulation of the stable isotope signal in Andean ice cores. *Journal of*
840 *Geophysical Research-Atmospheres* 108

841 Webster CR, Heymsfield AJ (2003) Water isotope ratios D/H, O-18/O-16, O-17/O-16 in
842 and out of clouds map dehydration pathways. *Science* 302:1742-1745

843 Werner M, Heimann M (2002) Modeling interannual variability of water isotopes in
844 Greenland and Antarctica. *Journal of Geophysical Research-Atmospheres*
845 107:4001, doi:4010.1029/2001JD900253

846 Werner M, Heimann M, Hoffmann G (2001) Isotopic composition and origin of polar
847 precipitation in present and glacial climate simulations. *Tellus* 53B:53-71

848 Williamson DL, Rasch PJ (1989) Two-dimensional semi-Lagrangian transport with shape
849 preserving interpolation. *Mon. Wea. Rev.* 117:102-129

850 Worden J, Noone D, Bowman K (2007) Importance of rain evaporation and continental
851 convection in the tropical water cycle. *Nature* 445:528-532

852 Yoshimura K, Kanamitsu M, Noone D, Oki T (2008) Historical isotope simulation using
853 reanalysis atmospheric data. *Journal of Geophysical Research Journal of*
854 *Geophysical Research*, 113, D19108, doi:10.1029/2008JD010074

855 Yung YL, Miller CE (1997) Isotopic fractionation of stratospheric nitrous oxide. *Science*
856 278:1778-1780

857

858 **Figure captions**

859 Fig 1: a) Percentage of precipitation that originated from evapotranspiration over a region
860 in South America (shown as bold box) deduced using a non-fractionating water tracking
861 scheme in the MUGCM, and b) the isotopic composition of that water. Adapted from
862 Noone and Simmonds (2002a).

863

864 Fig 2: Global model simulation of annual mean $\delta^{18}\text{O}$ in precipitation (‰) in a global
865 isotope model with a) fractionation only associated with surface evaporative sources and
866 dew/frost sinks, b) as in a) but with fractionation also associated with stratiform
867 condensation), c) as in a) but with fractionation also associated with convective
868 condensation, and d) the influence of fractionation during exchange as raindrops fall from
869 clouds. Panel b) and c) are differences relative to a), and panel d) is a difference relative
870 to a control simulation that has all fractionations, and is shown in Fig 4b. To the degree to
871 which the model results are linear, the (weighted) sum of all four components composes
872 the total isotope signal.

873

874

875

876

877

878

879 Fig 3: Schematic depiction of the third-generation isotope scheme describing the cloud
880 microphysics for isotopes used in CAM3 (adapted from Noone 2003). Detailed
881 exchanges between in-cloud properties and the environment, the accounting for multiple
882 microphysical moments, and inclusion of transport processes differentiates this scheme
883 from first and second generation schemes. Because on non-linearity in the budget
884 equations for the set of moments, such schemes usually need to be integrated
885 numerically.

886

887 Fig 4: Simulations of $\delta^{18}\text{O}$ in precipitation from three atmospheric models (MUGCM,
888 ECHAM and GISS) participating in the first Stable Water-isotope Intercomparison Group
889 (SWING) experiment, and from the observationally based regression model of Buenning
890 and Noone (2008). Contour interval is 4 ‰ with extra contours at -2 and 0 ‰. Shading in
891 panels b-d show where the models deviate from the GNIP data by more than 1 ‰. (red
892 positive and blue negative) with gradations of 1 ‰. (Courtesy N. Buenning 2008).

893

894 Fig 5: As in Fig 4 but for deuterium excess in precipitation. Contour interval is 1 ‰.
895 Light shading in panels b-d show where the models deviate from the observations by less
896 than -2 ‰, and dark shading shows where there differ by more than +2 ‰ with
897 gradations of 1 ‰. (Courtesy N. Buenning 2008).

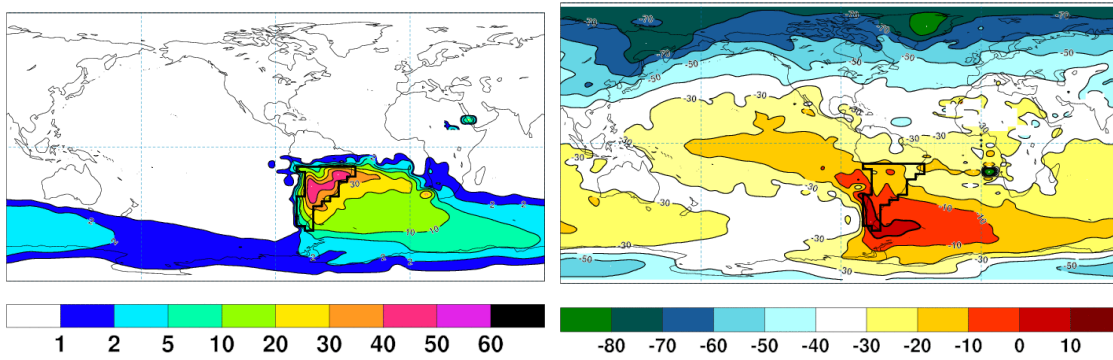
898

899

<i>Model</i>	<i>Reference</i>	<i>Domain</i>	<i>Type/resolution</i>	<i>Generation</i>
LMD	Joussaume et al., (1984). Joussaume and Jouzel (1991, 93)	Global	Finite difference	1 (2)
GISS 2'	Jouzel et al. (1987, 1991)	Global	Finite difference, 8x10 degree	1 (2)
Cloud model	Gedzelman and Arnold (1994). Lawrence et al. (1998)	Cloud scale	Two dimensional, 100m	1 (3)
ECHAM 3	Hoffman et al.(1998)	Global	Spectral/semi- Lagrangian T21/T42	2
ECHAM 4	Werner et al. (2001)	Global	Spectral/semi- Lagrangian T63/106	2
MUGCM	Noone and Simmonds (2002b)	Global	Spectral/semi- Lagrangian	1 (2)
GENESIS	Mathieu et al.(2002)	Global	Spectral/semi- Lagrangian T31	
CCM3	Noone (2003)	Global	Spectral/semi- Lagrangian T42	2
ICM	Yoshimura et al. (2003)?	Global 2d	Finite difference, offline, 1.25 degree	(1)
GISS E	Schmidt et al. (2005)	Global	Finite difference/quadratic moments, 4x5, 2x2.5	2 (3)
REMO	Sturm et al. (2007)	Regional	Finite difference 45 km, 10 km	2
CAM3	Noone (2003, 2006, in prep.)	Global	Finite volume 4x5, 2x2.5	3
DARMA	Smith et al, (2006)	Cloud scale	100 meter	4
CAM2	Lee et al. (2007)	Global	Spectral/semi- Lagrangian T42	2
CCSR/NIES	A. Numaguti (2005), Kurita in prep	Global	Spectral/semi- Lagrangian T42	2
GSM	Yoshimura et al. (2008)	Global	Spectral T62	2
RSM	Yoshimura, in prep	Regional	Spectral, 10-50 km	2
ECHAM 5	Harold et al., in prep	Global	To be finalized	2, or 3
LMD4	Risi et al. in prep	Global	To be finalized	2, or 3

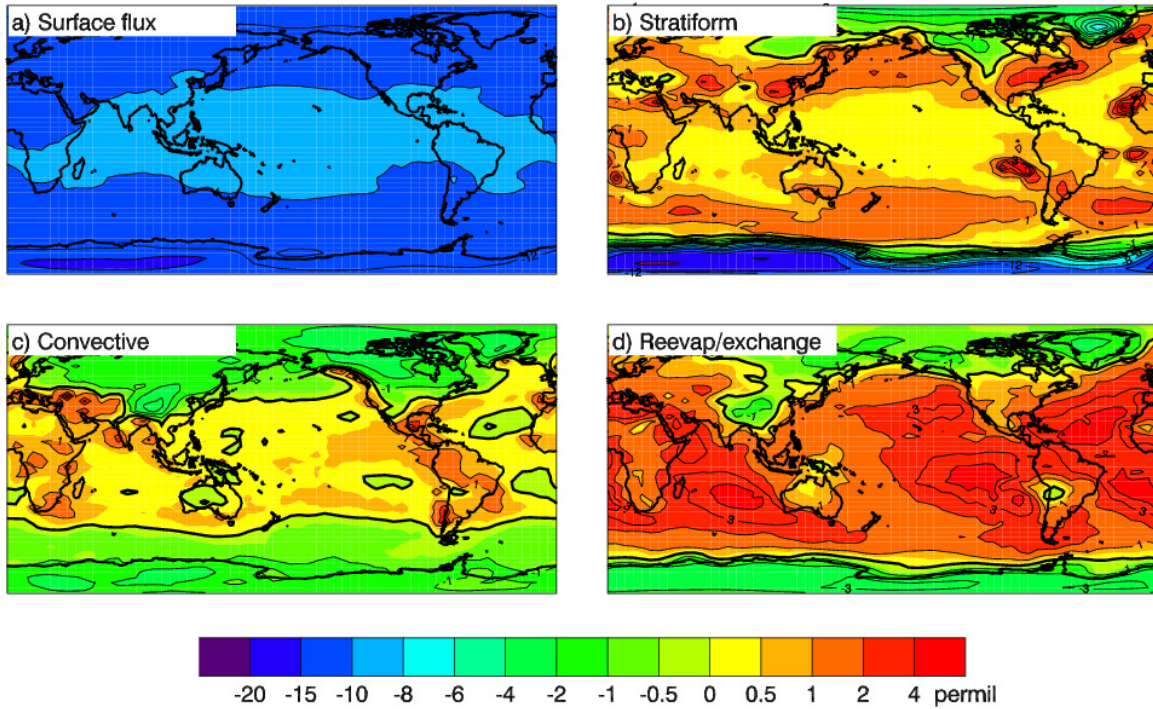
901 Table 1: Historical account of isotope models, in almost chronological order. Other
902 models reported to have isotope scheme being developed are the HadGem, UKMO,
903 ACCESS and WRF (Noone, personal communication, 2007, 2008). Generation number
904 in parentheses indicates the model is close to being classed at the higher level.

905



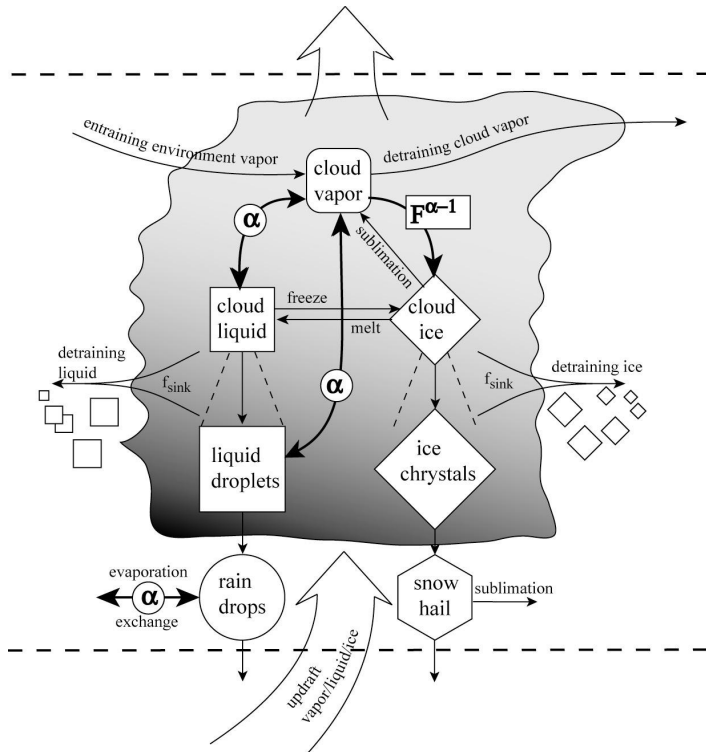
906

907 Fig 1: a) Percentage of precipitation that originated from evapotranspiration over a region
908 in South America (shown as bold box) deduced using a non-fractionating water tracking
909 scheme in the MUGCM, and b) the isotopic composition of that water. Adapted from
910 Noone and Simmonds (2002a).



912

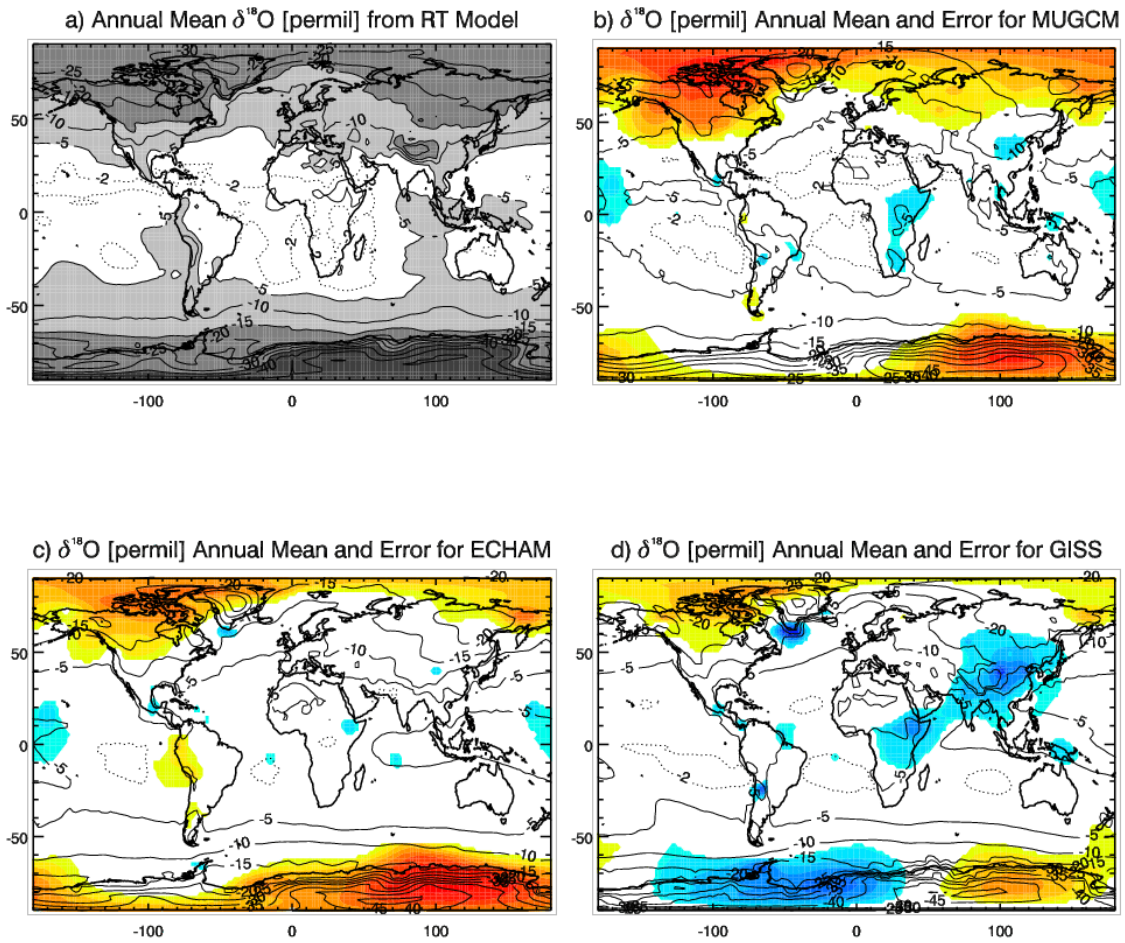
913 Fig 2: Global model simulation of annual mean $\delta^{18}\text{O}$ in precipitation (‰) in a global
 914 isotope model with a) fractionation only associated with surface evaporative sources and
 915 dew/frost sinks, b) as in a) but with fractionation also associated with stratiform
 916 condensation), c) as in a) but with fractionation also associated with convective
 917 condensation, and d) the influence of fractionation during exchange as raindrops fall from
 918 clouds. Panel b) and c) are differences relative to a), and panel d) is a difference relative
 919 to a control simulation that has all fractionations, and is shown in Fig 4b. To the degree to
 920 which the model results are linear, the (weighted) sum of all four components composes
 921 the total isotope signal.



923

924 Fig 3: Schematic depiction of the third-generation isotope scheme describing the cloud
 925 microphysics for isotopes used in CAM3 (adapted from Noone 2003). Detailed
 926 exchanges between in-cloud properties and the environment, the accounting for multiple
 927 microphysical moments, and inclusion of transport processes differentiates this scheme
 928 from first and second generation schemes. Because on non-linearity in the budget
 929 equations for the set of moments, such schemes usually need to be integrated
 930 numerically.

931



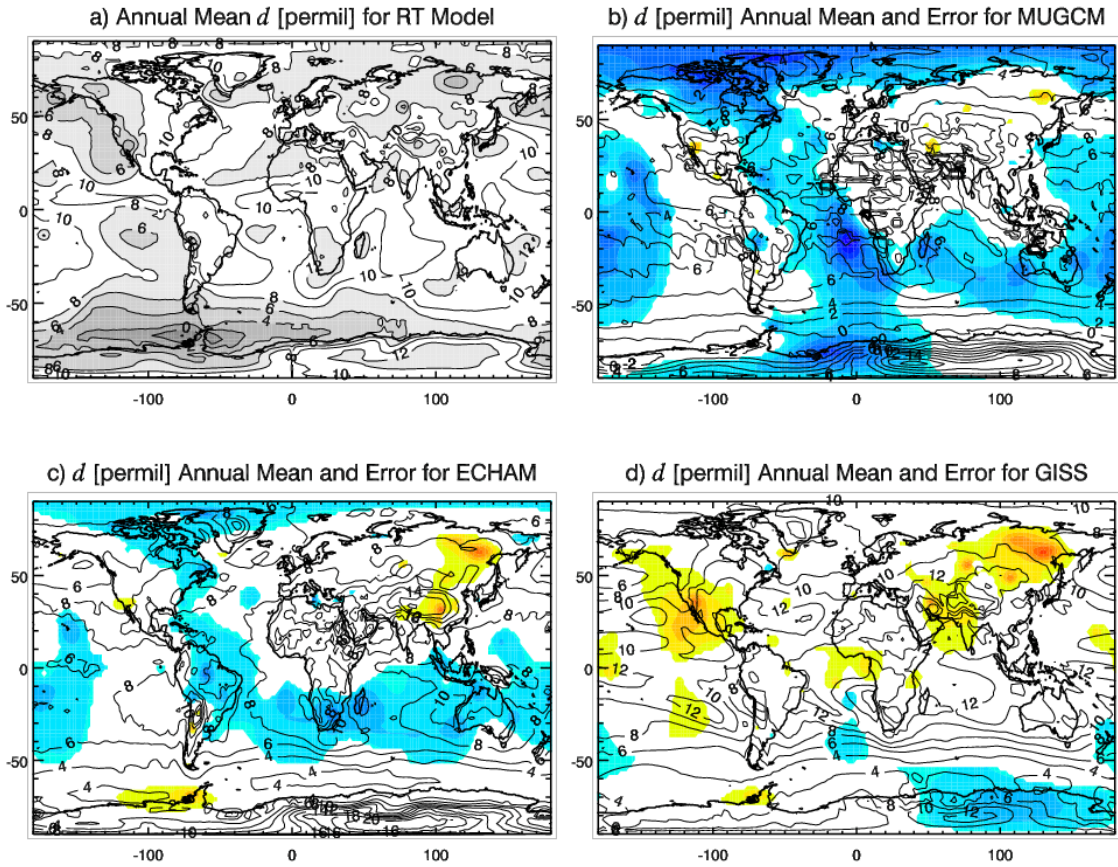
932

933

934

935 Fig 4: Simulations of $\delta^{18}\text{O}$ in precipitation from three atmospheric models (MUGCM,
936 ECHAM and GISS) participating in the first Stable Water-isotope Intercomparison Group
937 (SWING) experiment, and from the observationally based regression model of Buenning
938 and Noone (2008). Contour interval is 4 ‰ with extra contours at -2 and 0 ‰. Shading in
939 panels b-d show where the models deviate from the GNIP data by more than 1 ‰. (red
940 positive and blue negative) with gradations of 1 ‰. (Courtesy N. Buenning 2008).

941



942

943

944 Fig 5: As in Fig 4 but for deuterium excess in precipitation. Contour interval is 1 ‰.

945 Light shading in panels b-d show where the models deviate from the observations by less

946 than -2 ‰, and dark shading shows where there differ by more than +2 ‰ with

947 gradations of 1‰. (Courtesy N. Buenning 2008).

948

949

950

951